Published in final edited form as:
J Am Coll Cardiol. 2010 August 31; 56(10): 805–812. doi:10.1016/j.jacc.2010.03.070.

Calcium Dynamics and the Mechanisms of Atrioventricular Junctional Rhythm

Daehyeok Kim, MD, PhD, **Tetsuji Shinohara, MD, PhD**, **Boyoung Joung, MD, PhD**, **Mitsunori Maruyama, MD, PhD**, **Eue-Keun Choi, MD, PhD**, **Young Keun On, MD, PhD**, **Seongwook Han, MD, PhD**, **Michael C. Fishbein, MD***, **Shien-Fong Lin, PhD**, and **Peng-Sheng Chen, MD**

*Krannert Institute of Cardiology and the Division of Cardiology, Department of Medicine, Indiana University School of Medicine, Indianapolis, Indiana and Department of Pathology and Laboratory Medicine, UCLA, Los Angeles, CA

Abstract

Objectives—To test the hypothesis that rhythmic spontaneous sarcoplasmic reticulum (SR) calcium (Ca) release (the "Ca clock") plays an important role in atrioventricular junction (AVJ) automaticity.

Background—The AVJ is a primary backup pacemaker to the sinoatrial node. The mechanisms of acceleration of AVJ intrinsic rate during sympathetic stimulation are unclear.

Methods—We simultaneously mapped transmembrane potential (V_m) and intracellular Ca (Ca_i) in Langendorff-perfused canine AVJ preparations that did not contain sinoatrial node (N=10).

Results—Baseline AVJ rate was 37.5 ± 4.0 bpm. The wavefront from leading pacemaker site propagated first through the slow pathway, then the fast pathway and atria. There was no late diastolic Ca elevation (LDCAE) at baseline. Isoproterenol up to 3 μmol/L increased heart rate to 100 ± 6.8 bpm, concomitant with the appearance of LDCAE that preceded the phase 0 of action potential by 97.3 ± 35.2 ms and preceded the onset of late diastolic depolarization by 23.5 ± 3.5 ms. Caffeine also produced LDCAE and AVJ acceleration. The maximal slope of LDCAE and diastolic depolarization always co-localized with the leading pacemaker sites. Ryanodine markedly slowed the rate of spontaneous AVJ rhythm. Isoproterenol did not induce LDCAE in the presence of ryanodine. The I_f blocker ZD 7288 did not prevent LDCAE or AVJ acceleration induced by isoproterenol (N=2).

Conclusions—Isoproterenol and caffeine induced LDCAE and accelerated intrinsic AVJ rhythm. Consistent co-localization of the maximum LDCAE and the leading pacemaker sites indicates that Ca clock is important to the intrinsic AVJ rate acceleration during sympathetic stimulation.

Keywords

Automaticity; sympathetic stimulation; optical mapping; electrophysiology; arrhythmia

The mechanisms of automaticity have traditionally been attributed to the actions of multiple time- and voltage-dependent membrane ionic currents. However, recent studies showed that in addition to these membrane ionic clocks, rhythmic spontaneous sarcoplasmic reticulum (SR) Ca release (the Ca clock) can result in rhythmic I_{NCX} activation and SAN

Corresponding author: Peng-Sheng Chen, MD, 1801 N. Capitol Ave, E475, Indianapolis, IN 46202. Phone : 317-962-9755, Fax: 317-962-0588 chenpp@iupui.edu.

depolarization (1,2). We (3) recently confirmed that the membrane ionic clock worked synergistically with the Ca clock to generate sinus rhythm in dogs. Whether or not Ca clock contributed to heart rhythm generation in other parts of the heart was unclear. Atrioventricular junction (AVJ) contains specialized conduction tissues, including proximal AV bundle, His bundle and AV node (4). These specialized structures may participate in AVJ automaticity (5). The AVJ is also a common source of cardiac arrhythmia. However, relatively little is known about the mechanisms of automaticity in the AVJ. It has been demonstrated that I_{NCX} is present in cells from rabbit atrioventricular node (AVN), and removal of external Na produced a rise of intracellular Ca (Ca_i) through the reverse mode of I_{NCX} (6,7). It is also known that the rate of spontaneous activity of myocytes isolated from rabbit AVN may be decreased by ryanodine and increased by isoproterenol. These changes are accompanied by a decrease and an increase, respectively, in the slope of the preceding Ca ramp (8). These findings suggest that subcellular Ca_i dynamics (the “Ca clock”) may contribute to the automaticity of the AVJ. However, this hypothesis has not been tested in intact AVJ preparations. We hypothesize that Ca clock is important in AVJ automaticity in intact canine AVJ preparations, and that isoproterenol accelerate AVJ rhythm through the increased magnitude of SR Ca release. The purpose of this study is to perform simultaneous V_m and Ca_i mapping to test these hypotheses in a canine model.

Methods

This study protocol was approved by the Institutional Animal Care and Use Committee of Indiana University. Hearts from 10 normal mongrel dogs were excised under general anesthesia and were perfused through the aorta with cardioplegic solution. The proximal right and left circumflex arteries were separately cannulated (9). The AVJ preparations (Figure 1A) were perfused with Tyrode's solution at 37°C with 95% O_2 and 5% CO_2 to maintain a pH of 7.4 through the coronary cannula. The composition of Tyrode's solution (in mmol/L) was NaCl 125, KCl 4.5, NaH_2PO_4 1.8, $NaHCO_3$ 24, $MgCl_2$ 0.5, $CaCl_2$ 1.8 and glucose 5.5. Albumin 100 mg/L was added in deionized water. Contractility was inhibited by 10-17 μmol/L of blebbistatin. Pseudo-ECG was recorded with bipolar electrodes in right atrium. A multipolar electrophysiological catheter was used to record the His bundle electrogram,

Optical mapping

We performed simultaneous dual optical mapping of V_m and Ca_i while the hearts were Langendorff perfused (3). After mapping of baseline spontaneous beats, pharmacologic intervention was performed. All 10 hearts were mapped both at baseline and during pharmacologic intervention. Among them, 4 were used for β-adrenergic stimulation with Isoproterenol. In 2 hearts, ryanodine (3 μmol/L) was used without and with isoproterenol (1 μmol/L) infusion. In the remaining 4 hearts, we performed the following pharmacologic interventions: caffeine infusion (20 mmol/L given as a bolus in 1 s, N=2), ZD 7288 (3 μmol/L) followed by isoproterenol (1 μmol/L, N=2).

Histology

The tissues were fixed in formalin and the AVJ region was sectioned into five rectangular blocks as described by Inoue and Becker (10). The tissues were paraffin embedded, sectioned and stained with hematoxylin and eosin and with Masson's trichrome stain. In addition, we performed immunostaining of HCN4 with rabbit anti-HCN4 polyclonal antibody (Santa Cruz Biotechnology Inc, Santa Cruz, CA, USA).

Data analysis

The Ca_i and V_m traces were normalized to their respective peak-to-peak amplitude for comparison of timing and morphology. We assign the maximum amplitude of Ca_i and V_m during baseline pacing as one (1) arbitrary unit (AU). The amplitude and the slope of the late diastolic Ca elevation (LDCAE) were expressed as AU and AU/s, respectively (3). The same applies to diastolic depolarization detected on the V_m tracings. To generate an isochronal map, the optical mapping data were spatiotemporally filtered with a 3×3×3 moving average operation. The activation time at each pixel was determined by threshold crossing, usually set at the mid-point of the optical action potential. The activation isochrones were then constructed by grouping the pixels with the same activation time. Paired t-tests were used to compare the means at baseline and during pharmacologic intervention in the same preparation. ANOVA with Bonferroni post hoc test was used to compare the slopes of LDCAE and DD at different distances and with different doses of isoproterenol. Data were presented as mean ± SEM. A probability value of ≤0.05 was considered statistically significant.

Results

Anatomy of the AVJ

A picture of the AVJ preparation is shown in Figure 1A. The rectangle in the left panel was enlarged and shown at the right. The optical signals during atrial pacing (600 ms cycle length) at different sites are shown in Panel B. The locations of the fast pathway (FP), slow pathway (SP), transitional zone (TZ) and AVN were determined both by its anatomical locations (10) and by the characteristics of their optical signals (9). Specifically, the AVN was identified as sites with slow phase 0 with a notch (arrow) that corresponded temporally with the His potential registered by an electrophysiological catheter in the His area (bottom tracing). The location of the AVN was confirmed microscopically (red arrow, Figure 1C). The HCN4 staining was positive in the AVN and negative in the surrounding tissues (Figure 1D).

Characterization of AVJ Rhythm

Baseline AVJ rhythm had a rate of 37.5±4.0 bpm. Figure 2A shows the mapped region. Among them, sites a, b and c corresponded to the anatomical location of the AVN. Figure 2B shows the isochronal activation map of a single beat during the typical AVJ rhythm, with the earliest activation in the leading pacemaker site as time zero. In the all cases at baseline, the AVJ rhythm began near AVN and slowly propagated towards slow pathway region inferior to AVJ (Figure 2B, upper panel), and then rapidly propagates towards the other parts of the atrium (Figure 2B, lower panel). In this example, the former portion of the propagation took 130 ms and the latter portion only 15 ms (from 130 ms to 145 ms). There was an obvious conduction delay between AVN region and the rest of the RA preparation. Figure 2C shows the optical signals recorded at different sites shown in Figure 2B. There was diastolic depolarization (arrows) at the leading pacemaking site near AVN. These diastolic depolarizations occurred without preceding LDCAE on the Ca_i tracing. Panel 2D shows these optical signals in greater detail. The upstroke slope of optical V_m and Ca_i fluorescence was shallow in the AVN and the slow pathway (sites ad). There was very slow propagation between sites c and f. The propagation from f to i was fast, and was associated with a steep slope in the phase 0. The delay between phase 0 of site c and phase 0 of site f in all preparations averaged 102 ± 25.5 ms.

Effects of Pharmacological Interventions

β-adrenergic stimulation—Isoproterenol increased the rate of AVJ rhythm in a dose-dependent fashion from 0.01 to 3.0 μmol/L (Figure 3A). In all preparation studied, the heart rate increased by a maximum of 167.2% (from 37.5 ± 4.0 bpm to 100.2 ± 6.8 bpm) during isoproterenol infusion. The slope of DD progressively decreased as the distance between the recording site and the leading pacemaker site progressively increased (Figure 3B). We also noted that LDCAE appeared at the leading pacemaker sites in the all 6 preparations during isoproterenol infusion (arrow, Figure 3C). LDCAE at the leading pacemaker site preceded the phase 0 action potential upstroke by 97.3±35.2 ms and preceded the onset of late diastolic depolarization by 23.5 ± 3.5 ms (Figure 3D). Similar to diastolic depolarization, the slope of LDCAE progressively decreased as the distance from pacing site increased (Figure 3B). In this (Figure 3C) and an additional 3 preparations, the same site served as the leading pacemaker both at baseline and during isoproterenol infusion. In 4 preparations, however, the leading pacemaker sites shifted during isoproterenol infusion. At the leading pacemaker sites, the slopes (AU/s) of LDCAE are 0, 1.47±0.16, 2.04±0.18, 2.93±0.18, 3.38±0.27 and 4.00±0.21 with 0 μmol/L, 0.01 μmol/L, 0.03 μmol/L, 0.1 μmol/L, 0.3 μmol/L and 1.0 μmol/L of isoproterenol, respectively ($P<0.001$). The slopes of DD (AU/s) are 0, 0.55±0.15, 0.95±0.16, 1.40±0.15, 1.93±0.10 and 2.28±0.10 with 0 μmol/L, 0.01 μmol/L, 0.03 μmol/L, 0.1 μmol/L, 0.3 μmol/L, 1.0 μmol/L of isoproterenol, respectively ($P<0.001$). Posthoc tests showed that there were significant differences among all groups with p values ranging from 0.000 to 0.001 for LDCAE and from 0.000 to 0.0038 for DD.

Figure 4A summarizes the responses to isoproterenol of all preparations studied. Arrows in Figure 4A shows the original leading pacemaker site (filled black dots) and the leading pacemaking sites during isoproterenol infusion (unfilled black dots). The filled red dots indicate sites where there were no shifts. Figure 4B shows the isochronal activation maps and the corresponding Ca_i maps of preparation labeled “3” in Figure 4A. The baseline activation originated in the AVN region (site a, blue color). The activation then shifted downward with 0.01 μmol/L isoproterenol (site b). Further increase of dose to 0.1 μmol/L resulted in a leftward shift to site c. Figure 4C shows that the sites of LDCAE (arrows) shifted along with the leading pacemaker site. In all 4 preparations with shifting leading pacemaker sites, the LCDAE always co-localized with the leading pacemaker site.

Caffeine—We gave caffeine as a 2-mL bolus (20 mmol/L) directly into the left circumflex artery in 2 preparations. Figure 5A shows the direction of impulse propagation (arrows) along the slow and fast pathways. Figures 5B and 5C show Ca_i and V_m tracings along the slow pathway (SP) and fast pathway (FP), respectively, during caffeine infusion. Arrows point to LDCAE at the leading pacemaker (LP) site. Figure 5D shows actual V_m and Ca_i recorded at baseline and during caffeine infusion at leading pacemaker (LP), fast pathway (FP) and slow pathway (SP). The slopes of LDCAE (3.25±0.14 AU/s) and DD (2.41±0.05 AU/s) during caffeine infusion are significantly steeper than LDCAE and DD at baseline (0 AU/s, $p=0.020$ and 0.27±0.16 AU/s, $p=0.022$, respectively). LDCAE (arrows) appeared in the leading pacemaker site and the mean AVJ rate increased by 108 % (from 37.5±4.0 to 78.3±3.2 bpm). In these 2 preparations, the leading pacemaker sites did not shift locations during caffeine infusion. Similar to that seen during Isoproterenol infusion, the sites with maximum slopes of LDCAE and diastolic depolarization always co-localized with the leading pacemaker sites. The slopes decreased progressively as the recording sites moved away from the leading pacemaker site (Figure 5E).

Ryanodine—Figure 6 shows the effects of ryanodine in one preparation. Ryanodine 3 μmol/L markedly slowed the rate of spontaneous AVJ rhythm by 83.2% from 37.5 ± 4.0 to 6.3 ± 6.2 bpm (Figure 6A). Isoproterenol infusion after ryanodine (N=2) increased the heart

rate only to 16.4 ± 6.3 bpm, which was 56.2 % less than the baseline rate before ryanodine (Figure 6A). Figure 6B shows that ryanodine reduced the AVJ rate in a preparation receiving isoproterenol infusion. Isoproterenol did not induce LDCAE in the presence of ryanodine, and the heart rate increase was not associated with LDCAE (Figure 6C).

ZD 7288—The I_f blocker ZD 7288 (3 μmol/L) decreased basal AVJ rate by 35 % (n=2). The ZD 7288 did not prevent 1.0 μmol/L isoproterenol from increasing AVJ rate by 158 % (p =0.011, compared with basal rate), accompanied by the appearance of LDCAE with leading pacemaker shifted to the upper site in the AVN. There was apparent LDCAE at the leading pacemaker site (Figure 7B).

Discussion

The present study shows that isoproterenol and caffeine-induced AVJ rhythm acceleration was accompanied by increased LDCAE. The isoproterenol effects were suppressed by ryanodine but not by ZD 7288. There was co-localization of the maximum LDCAE with the leading pacemaking sites in the AVJ. These findings suggest that spontaneous SR Ca release plays an important role in the mechanisms of AVJ rate acceleration during isoproterenol or caffeine infusion. A functioning Ca clock in the AVJ is important to the generation of heart rhythm when sinoatrial node is impaired or not present.

Mechanisms of AVJ Rhythm

Whether or not the studies of SAN can be directly applied to the mechanisms of AVJ rhythm acceleration during isoproterenol infusion is unclear. Because the AVN and posterior extension express HCN4 (channel responsible for I_f), it is plausible to hypothesize that I_f is responsible for the AVJ automaticity (11). The present study shows that in addition to I_f and the membrane voltage clock, the Ca clock is also important in AVJ automaticity. Unlike SAN, the anatomic location of the AVJ pacemaker in rabbit heart is stable during autonomic modulation (12). Consistent with that finding, the leading pacemaker sites in a majority of preparations in our study do not move during isoproterenol infusion. However, in four preparations, the leading pacemaker sites do move with isoproterenol. More importantly, simultaneous Ca_i and V_m mapping showed that LDCAE preceded the onset of late diastolic depolarization, and that the leading pacemaking site always co-localized with the maximum slope of the LDCAE. Ryanodine was more effective than ZD 7288 in preventing heart rate acceleration induced by isoproterenol. Ridley et al (8) isolated myocytes from AVN of the rabbit hearts and performed optical mapping of the Ca_i transients in those myocytes. They found that there are spontaneous Ca_i transients in the AVN cells. These transients ramped up the amplitude prior to the onset of the upstroke of the Ca_i. The morphology of the Ca_i ramp in that study was the same as the LDCAE at the leading pacemaker sites in the present study. The authors also reported the ryanodine inhibited the spontaneous Ca_i transients and reduced the rates of spontaneous activation. Our study extended their observations to the intact AVJ. The availability of simultaneous V_m signals confirmed that these Ca_i ramps described by Ridley et al in fact occurred prior to the onset of the phase 0 of the action potential. Taken together, these data indicate that SR Ca clock plays an important role in AVJ automaticity.

Study limitations

Optical signals collected from the canine 3-D tissues represent a weighted average of the transmembrane action potentials throughout the entire canine atrial wall (19). It is possible that the little foot in front of the optically recorded action potential or Ca_i transients is not DD or LDCAE, but rather a strongly filtered optical recording from the deeper structures. However, as shown in Figure 4C, the site of Ca_i elevation moves from one site to another

during isoproterenol infusion, and it always co-localizes with the earliest site of activation on the isochronal map. Similarly, the DD in leading pacemaker site occurs during isoproterenol infusion but not at baseline (Figure 3C). These findings rule out a fixed deeper structure as a source of these isoproterenol-induced deflections.

Because of the complex origin of the impulse near the AVJ, it is possible that activation propagated from the SAN might contaminate the signals of the AVJ (13). Therefore, we trimmed away the sinus node in the present study, allowing the impulse originated from AVJ itself to propagate towards the surrounding atrial myocardium. The late diastolic depolarization and the first action potential upstroke observed in the AJV region therefore represent signals initiated in the AVJ. The second upstroke in the optical signal represents the signals of a different layer (the non-pacemaking atrial myocardium) that was excited by the AVJ pacemaker. We propose that late diastolic depolarization and LDCAE are not affected by the activations of non-pacemaking cells in this study.

Acknowledgments

We thank Jian Tan, Yanhua Zhang and Lei Lin for their assistance.

Supported by the NIH/NHLBI grants P01 HL78931, R01 HL78932, 71140, a Korean Ministry of Information and Communication through research and develop support project (BJ), a Nihon Kohden/St Jude Medical electrophysiology fellowship (MM), a Piansky Family Endowment (MCF), an AHA Established Investigator Award (SFL) and a Medtronic-Zipes Endowment (PSC).

Medtronic Inc and Cryocath Inc donated research equipment.

Abbreviations

AU	arbitrary unit
AVJ	atrioventricular junction
AVN	atrioventricular node
Ca_i	intracellular calcium
FP	fast pathway
HCN4	Hyperpolarization activated cyclic nucleotide-gated potassium channel 4
I	membrane ionic current
LDCAE	late diastolic calcium elevation
SAN	sinoatrial node
SR	sarcoplasmic reticulum
SP	slow pathway
TZ	transitional zone
V_m	transmembrane potential

References

1. Lakatta EG, Vinogradova T, Lyashkov A, et al. The integration of spontaneous intracellular Ca2+ cycling and surface membrane ion channel activation entrains normal automaticity in cells of the heart's pacemaker. Ann.N.Y.Acad.Sci 2006;1080:178–206. [PubMed: 17132784]
2. Maltsev VA, Lakatta EG. Synergism of coupled subsarcolemmal Ca2+ clocks and sarcolemmal voltage clocks confers robust and flexible pacemaker function in a novel pacemaker cell model. Am.J.Physiol Heart Circ.Physiol 2009;296:H594–H615. [PubMed: 19136600]

3. Joung B, Tang L, Maruyama M, et al. Intracellular calcium dynamics and acceleration of sinus rhythm by beta-adrenergic stimulation. Circulation 2009;119:788–796. [PubMed: 19188501]
4. Racker DK, Kadish AH. Proximal atrioventricular bundle, atrioventricular node, and distal atrioventricular bundle are distinct anatomic structures with unique histological characteristics and innervation. Circulation 2000;101:1049–59. [PubMed: 10704174]
5. Racker DK. Sinoventricular transmission in 10 mM K+ by canine atrioventricular nodal inputs. Superior atrionodal bundle and proximal atrioventricular bundle. Circulation 1991;83:1738–53. [PubMed: 1850667]
6. Convery MK, Hancox JC. Na+-Ca2+ exchange current from rabbit isolated atrioventricular nodal and ventricular myocytes compared using action potential and ramp waveforms. Acta Physiol Scand 2000;168:393–401. [PubMed: 10712577]
7. Hancox JC, Levi AJ, Brooksby P. Intracellular calcium transients recorded with Fura-2 in spontaneously active myocytes isolated from the atrioventricular node of the rabbit heart. Proc.Biol.Sci 1994;255:99–105. [PubMed: 8165231]
8. Ridley JM, Cheng H, Harrison OJ, et al. Spontaneous frequency of rabbit atrioventricular node myocytes depends on SR function. Cell Calcium 2008;44:580–591. [PubMed: 18550162]
9. Wu J, Olgin J, Miller JM, Zipes DP. Mechanisms underlying the reentrant circuit of atrioventricular nodal reentrant tachycardia in isolated canine atrioventricular nodal preparation using optical mapping. Circ.Res 2001;88:1189–1195. [PubMed: 11397786]
10. Inoue S, Becker AE. Posterior extensions of the human compact atrioventricular node: a neglected anatomic feature of potential clinical significance. Circulation 1998;97:188–193. [PubMed: 9445172]
11. Hucker WJ, Nikolski VP, Efimov IR. Optical mapping of the atrioventricular junction. J Electrocardiol 2005;38:121–5. [PubMed: 16226086]
12. Hucker WJ, Nikolski VP, Efimov IR. Autonomic control and innervation of the atrioventricular junctional pacemaker. Heart Rhythm 2007;4:1326–35. [PubMed: 17905339]
13. Efimov IR, Mazgalev TN. High-resolution, three-dimensional fluorescent imaging reveals multilayer conduction pattern in the atrioventricular node. Circulation 1998;98:54–57. [PubMed: 9665060]
14. Nikolski V, Efimov I. Fluorescent imaging of a dual-pathway atrioventricular-nodal conduction system. Circ.Res 2001;88:E23–E30. [PubMed: 11179207]
15. Baxter WT, Mironov SF, Zaitsev AV, Jalife J, Pertsov AM. Visualizing excitation waves inside cardiac muscle using transillumination. Biophysical Journal 2001;80:516–530. [PubMed: 11159422]
16. de Bakker JM, Loh P, Hocini M, Thibault B, Janse MJ. Double component action potentials in the posterior approach to the atrioventricular node: do they reflect activation delay in the slow pathway? J.Am.Coll.Cardiol 1999;34:570–577. [PubMed: 10440175]
17. McGuire MA, de Bakker JMT, Vermeulen JT, Opthof T, Becker AE, Janse MJ. Origin and significance of double potentials near the atrioventricular node. Correlation of extracellular potentials, intracellular potentials, and histology. Circulation 1994;89:2351–2360. [PubMed: 8181161]
18. Loh P, de Bakker JM, Hocini M, Thibault B, Hauer RN, Janse MJ. Reentrant pathway during ventricular echoes is confined to the atrioventricular node: high-resolution mapping and dissection of the triangle of koch in isolated, perfused canine hearts. Circulation 1999;100:1346–53. [PubMed: 10491381]
19. Fedorov VV, Schuessler RB, Hemphill M, et al. Structural and functional evidence for discrete exit pathways that connect the canine sinoatrial node and atria. Circ.Res 2009;104:915–923. [PubMed: 19246679]

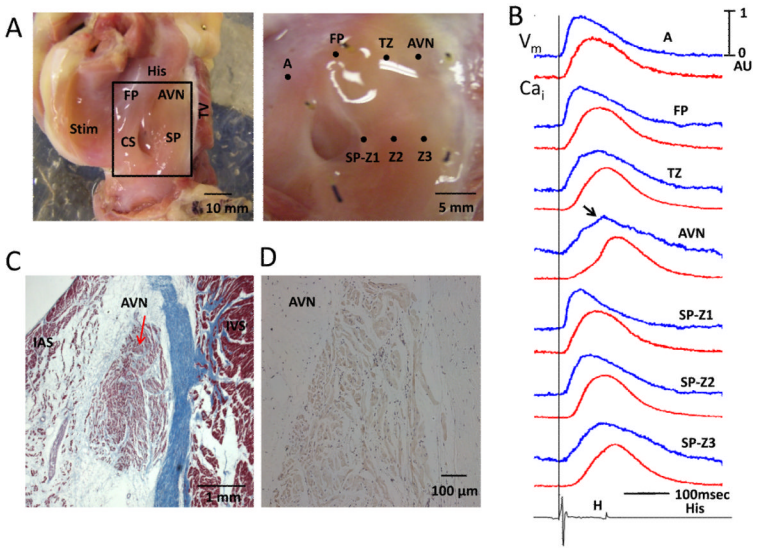

Figure 1.

Gross anatomy and histology of the AVJ preparation. A, left panel shows the AVJ preparation used in the study. Area outlined by the rectangle was the area mapped. The right panel shows the area mapped in greater detail. The optical signals from the labeled sites are shown in Panel B. The blue line is the optical V_m while the red line is optical Ca_i tracing. Arrow points to an additional hump on the AVN, which corresponded to the His bundle potential on the bottom of the Panel B. A vertical line indicates the beginning of atrial pacing spike. The pacing cycle length was 600 ms. C, Histology of a transmural section through the AVN (arrow). The slide was stained with Masson's trichrome stain (×100). Panel D shows positive (brown) immunostaining of HCN4 in the AVN but not in the surrounding tissues. AVN, atrioventricular node; CS, coronary sinus; FP, fast pathway; IAS, interatrial septum; IVS, interventricular septum; SP, slow pathway; TV, Tricuspid valve; TZ, transitional zone; SP-Z1, 2 and 3 indicates slow pathway zones 1, 2 and 3, respectively.

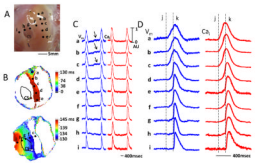

Figure 2.

Optical recording during spontaneous AVJ rhythm. A, Filled circles represent optical recording sites. ‘a’ indicates the earliest activation site. B, Isochronal activation map during spontaneous AVJ rhythm shows slow conduction towards the area between CS and tricuspid valve. After a delay, the wavefront conducted rapidly away and excited the entire atrium. C, Optical V_m (blue) and Ca_i (red) tracings during spontaneous AVJ rhythm. Arrows point to phase 4 diastolic depolarization near the AVN. D shows the same tracings in greater detail. The vertical dashed line ‘j’ indicates the time of action potential onset at site a. The vertical dashed line ‘k’ indicates the time of action potential onset at site i.

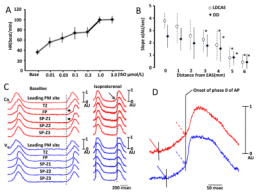

Figure 3.

Effects of isoproterenol. A, Dose-response relationship between heart rate (HR) and isoproterenol (ISO). B, The relationship between the slope and distance from the leading pacemaker (LP) site for late diastolic Ca elevation (LDCAE) and diastolic depolarization (DD). Asterisks indicate significant difference ($P \leq 0.05$) between the slopes at the EAS and at sites distant from EAS. C, The Ca_i (red) and V_m (blue) tracings at baseline and during isoproterenol infusion. At baseline, the initial portions of the FP and SP-Z1 (indicated by asterisks) showed gradual rise of V_m, suggesting that these sites have recorded optical signals from anatomical layers that activated earlier. During isoproterenol infusion, LDCAE (arrow) occurred before phase 0 (vertical dashed line) of the leading pacemaker. D, Magnified view of Ca_i and V_m tracings of AVN during isoproterenol infusion. The onset of LDCAE (solid red arrow) was noted before the onset of AP (solid blue arrow). Red dashed arrow indicates peak LDCAE and blue dashed arrow indicate peak diastolic depolarization. The vertical line segment indicates the onset of the phase 0 of action potential. EAS, earliest activation site; PM, pacemaker.

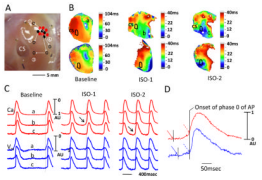

Figure 4.

Shift of leading pacemaker sites during isoproterenol infusion. A shows the directions of the shifts of all preparations. B, Isochronal activation maps showing shift of leading pacemaker site in heart #3 during isoproterenol infusion. The upper and lower parts were V_m and Ca_i isochronal activation maps, respectively. This case shows pacemaker shifts from baseline 'a' site to 'b' and then to 'c' site during isoproterenol infusion. C, Optical V_m and Ca_i recording in same case. D, Magnified view of Ca_i and V_m tracings of early activation site (C) at ISO-2. A robust LDCAE (arrow) always co-localized with leading pacemaker site. Vertical broken lines indicate the onset of action potential in the leading pacemaker site. The onset of LDCAE (solid red arrow) was noted before the onset of AP (solid blue arrow). Red dashed arrow indicates peak LDCAE and blue dashed arrow indicate peak diastolic depolarization. ISO-1 indicates an isoproterenol dose 0.01 μmol/L. ISO-2 indicates an isoproterenol dose of 0.1 μmol/L.

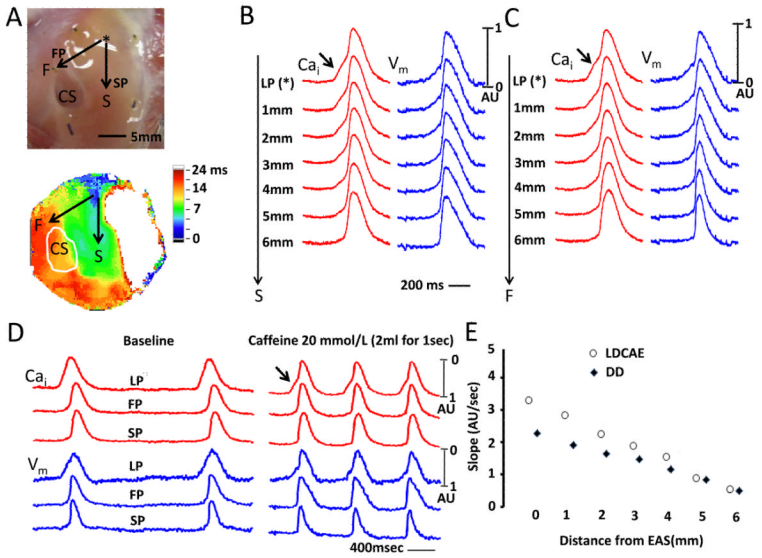

Figure 5.

Spatial changes of Ca_i(red) and V_m(blue) around the leading pacemaker site (asterisk) after caffeine injection. A, Upper panel shows the area mapped. The arrow along slow pathway (SP) is labeled S, while the arrow along the fast pathway (FP) is labeled F. Lower panel shows isochronal activation map after caffeine injection. B, The Changes of V_m and Ca_i tracings along slow pathway direction. C, The Changes of V_m and Ca_i tracings along fast pathway direction. D, The Ca_i (red) and V_m (blue) tracings at baseline and after caffeine injection. The arrow indicate LDCAE. E, The relationship between the slope and distance from the leading pacemaker (LP) site for LDCAE and DD. CS, coronary sinus; EAS, earliest activation site

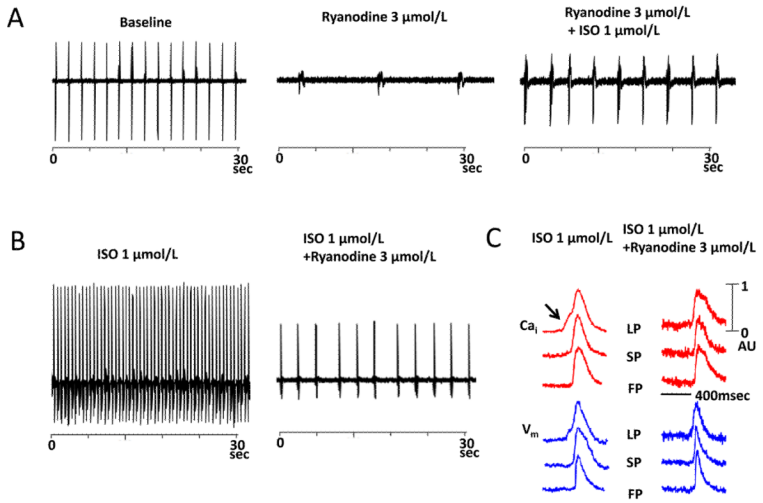

Figure 6.

The effect of ryanodine on automaticity of intact Canine AVN. A, Ryanodine 3 µmol/L markedly slowed the rate of AVJ rhythm by 83.2% (mid panel). Isoproterenol infusion after ryanodine increased the heart rate only to 16.4 ± 6.3 bpm (right panel). B shows that the effects of isoproterenol on heart rate were significantly suppressed by ryanodine. C, Effect of ryanodine on the isoproterenol-induced LDCAE. Ryanodine completely abolished the LDCAE (Arrow). LP, leading pacemaker; SP, slow pathway; FP, fast pathway; ISO, isoproterenol.

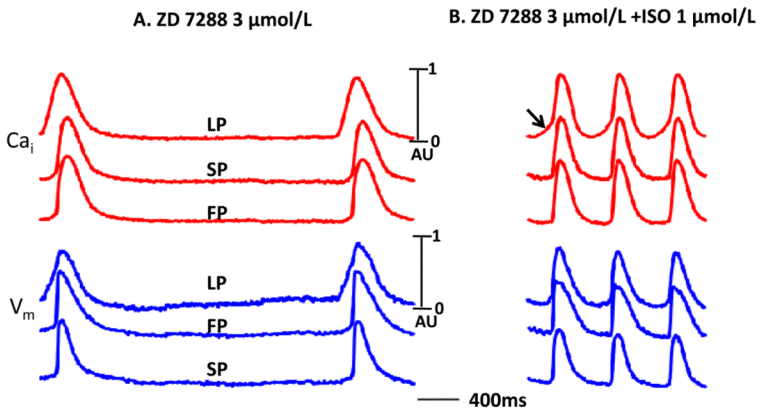

Figure 7.

The effect ZD 7288 on intact canine AVN. A. The Ca_i and V_m tracing during 3 µmol/L ZD 7288 infusion. B. Isoproterenol 1 µmol/L produced LDCAE (arrow) at the leading pacemaker site in the presence of ZD 7288. LP, leading pacemaker site; SP, slow pathway; FP, fast pathway; ISO, isoproterenol.